8-29-2023

Bcl6, Irf2, and Notch2 promote nonclassical monocyte development

Kevin W O'Connor
Washington University School of Medicine in St. Louis
Tiantian Liu
Washington University School of Medicine in St. Louis
Sunkyung Kim
Washington University School of Medicine in St. Louis
Carlos G Briseño
Washington University School of Medicine in St. Louis
Katia Georgopoulos
Harvard University

See next page for additional authors

Recommended Citation

O'Connor, Kevin W; Liu, Tiantian; Kim, Sunkyung; Briseño, Carlos G; Georgopoulos, Katia; Murphy, Theresa L; and Murphy, Kenneth M, "Bcl6, Irf2, and Notch2 promote nonclassical monocyte development." Proceedings of the National Academy of Sciences of the United States of America. 120, 35. e2220853120 (2023).
https://digitalcommons.wustl.edu/oa_4/3234

PNAS RESEARCH ARTICLE | IMMUNOLOGY AND INFLAMMATION

Bcl6, *Irf2*, and *Notch2* promote nonclassical monocyte development

Kevin W. O'Connor[a], Tiantian Liu[a], Sunkyung Kim[a], Carlos G. Briseño[a,1], Katia Georgopoulos[b], Theresa L. Murphy[a], and Kenneth M. Murphy[a,2]

Contributed by Kenneth M. Murphy; received December 7, 2022; accepted July 28, 2023; reviewed by Dan R. Littman and Miriam Merad

Ly6C^{lo} monocytes are a myeloid subset that specializes in the surveillance of vascular endothelium. Ly6C^{lo} monocytes have been shown to derive from Ly6C^{hi} monocytes. NOTCH2 signaling has been implicated as a trigger for Ly6C^{lo} monocyte development, but the basis for this effect is unclear. Here, we examined the impact of NOTCH2 signaling of myeloid progenitors on the development of Ly6C^{lo} monocytes in vitro. NOTCH2 signaling induced by delta-like ligand 1 (DLL1) efficiently induced the transition of Ly6C^{hi} TREML4^{-} monocytes into Ly6C^{lo} TREML4^{+} monocytes. We further identified two additional transcriptional requirements for development of Ly6C^{lo} monocytes. Deletion of BCL6 from myeloid progenitors abrogated development of Ly6C^{lo} monocytes. IRF2 was also required for Ly6C^{lo} monocyte development in a cell-intrinsic manner. DLL1-induced in vitro transition into Ly6C^{lo} TREML4^{+} monocytes required IRF2 but unexpectedly could occur in the absence of NUR77 or BCL6. These results imply a transcriptional hierarchy for these factors in controlling Ly6C^{lo} monocyte development.

nonclassical monocytes | Bcl6 | IRF2 | Notch2

Significance

Nonclassical monocyte development is poorly understood, inhibiting studies of their function and efforts to target them therapeutically. We identify BCL6 and IRF2 as transcription factors required for nonclassical monocytes in mice. We additionally develop a Notch-mediated system modeling nonclassical monocyte development in vitro. This work deepens our understanding of how nonclassical monocytes arise and will support future work assessing the function and therapeutic potential of this cell type.

Nonclassical monocytes are a unique subset of peripheral blood mononuclear cells (PBMCs) that function in surveillance of vascular endothelium (1, 2). Monocyte heterogeneity was originally observed by differing expression patterns of Fc receptors on human PBMCs (3). Later, two populations of human PBMCs were distinguished as either CD14^{hi} CD16^{-} or CD14^{dim} CD16^{+} cells (4). CD14^{dim} CD16^{+} cells, despite remaining in the circulation, exhibited features of tissue macrophages, such as high levels of MHC class II expression (5). Subsequent studies reported that CD14^{dim} CD16^{+} monocytes comprised 10% of PBMCs in healthy subjects, but were expanded in sepsis, HIV infection, and asthma (6–10).

Murine nonclassical monocytes were first identified using an EGFP reporter for CX_3CR1 (11), which described nonclassical monocytes as short-lived CX_3CR1^{hi} CCR2^{-} Gr1(Ly6C/G)$^{-}$ cells, in contrast to CX_3CR1^{lo} CCR2^{+} Gr1^{+} classical monocytes (12). Subsequent studies divided monocytes on the basis of Ly6C expression, with Ly6C^{hi} PBMCs being recently released from the bone marrow (BM) and losing Ly6C expression in the circulation (13). Nonclassical monocytes are distinguished not only by lack of Ly6C expression, but also by induction of TREML4 and CD11c expression (14). Nonclassical monocytes have been called "patrolling" monocytes based on their attachment to and movement along vascular endothelium (15). This movement is dependent on LFA-1 and independent of the direction of blood flow. Nonclassical monocytes serve to monitor and repair vascular endothelium (16) and can protect against tumor metastasis by engulfing tumor material and recruiting NK cells (17–19).

Ly6C^{hi} monocytes develop from the monocyte dendritic cell progenitor (MDP) (20, 21) through a committed monocyte progenitor (cMoP) (22, 23). Ly6C^{hi} monocytes require the transcription factors PU.1, KLF4, and IRF8 for their development, with PU.1 and IRF8 both functioning to promote KLF4 expression (24–27). Fate mapping studies identify Ly6C^{hi} classical monocytes as precursors of Ly6C^{lo} nonclassical monocytes (28). Additionally, Ly6C^{hi} monocytes give rise to Ly6C^{lo} monocytes in a congenic transfer model (29). This establishes Ly6C^{lo} monocytes as the product of a developmental pathway including MDPs, cMoPs, and Ly6C^{hi} monocytes.

Currently, three transcription factors, NUR77, C/EBPβ, and NOTCH2, have been identified that selectively regulate the development of Ly6C^{lo} monocytes. *Nr4a1* (NUR77) was observed to be selectively expressed highly in Ly6C^{lo} but not Ly6C^{hi} monocytes, and mice globally deficient in *Nr4a1* lacked Ly6C^{lo} but not Ly6C^{hi} monocytes (30). Loss of *Nr4a1* also results in excessive NF-kB activation in macrophages and defective formation of T cell tolerance (31, 32). The mechanism for the requirement of *Nr4a1* in Ly6C^{lo} monocytes is currently unclear. Deletion of an enhancer region located approximately 4 kb upstream of the *Nr4a1* promoter selectively eliminates Ly6C^{lo} monocytes without

Author affiliations: [a]Department of Pathology and Immunology, Washington University in St. Louis, School of Medicine, St. Louis, MO 63110; and [b]Cutaneous Biology Research Center, Massachusetts General Hospital, Harvard Medical School, Boston, MA 02114

Author contributions: K.W.O., C.G.B., T.L.M., and K.M.M. designed research; K.W.O., T.L., S.K., C.G.B., and T.L.M. performed research; K.W.O. and K.G. contributed new reagents/analytic tools; K.W.O., T.L., S.K., and C.G.B. analyzed data; and K.W.O., T.L.M., and K.M.M. wrote the paper.

Reviewers: D.R.L., NYU Langone Health; and M.M., Icahn School of Medicine at Mount Sinai.

The authors declare no competing interest.

[1]Present address: Department of Oncology, Amgen Inc., South San Francisco, CA 94080.

[2]To whom correspondence may be addressed. Email: kmurphy@wustl.edu.

This article contains supporting information online at https://www.pnas.org/lookup/suppl/doi:10.1073/pnas.2220853120/-/DCSupplemental.

Published August 22, 2023.

affecting macrophages (19). C/EBPβ is also selectively required for Ly6C^{lo} but not Ly6C^{hi} monocytes (29, 33, 34). The basis for this requirement is still somewhat uncertain, but may involve the reduction of M-CSF receptor (CD115/*Csf1r*) expression in *Cebpb*$^{-/-}$ mice (33) or a requirement for C/EBPβ to support the expression of *Nr4a1* (29). Finally, NOTCH2 signaling was suggested to induce the transition of Ly6C^{hi} monocytes into Ly6C^{lo} monocytes based on conditional *Notch2* deletion using *LysM*^{Cre} deletor strain (35). However, this study observed only a partial reduction in Ly6C^{lo} monocytes in vivo, which appeared to result from incomplete deletion of NOTCH2 in this system. The relationship between NUR77, C/EBPβ, and NOTCH2 in nonclassical monocytes remains unclear.

Here, we established an in vitro system to examine the development of Ly6C^{lo} monocytes. We show that Notch signaling in monocyte progenitors and Ly6C^{hi} monocytes rapidly induces the transition to Ly6C^{lo} monocytes. This transition can be mediated directly by expression of the Notch intracellular domain (NICD) but not by the expression of the Notch target HES1. In addition, we have identified two additional transcription factors required for Ly6C^{lo} monocyte development in vivo, *Bcl6*, and *Irf2*. The initial transition to a Ly6C^{lo} monocyte phenotype induced by Notch requires *Irf2* but occurs independently of *Bcl6* and *Nr4a1*. These results suggest that these factors play distinct roles in either the initial induction or survival of Ly6C^{lo} monocytes.

Results

Ly6C and TREML4 Identify Nonclassical Monocytes In Vivo and In Vitro. We wished to establish an in vitro protocol to examine genetic epistasis of nonclassical monocyte development. A previous study treated Ly6C^{hi} monocytes in vitro with a DLL1-Fc fusion protein to examine the development of nonclassical monocytes (35). However, this analysis did not test TREML4 as a marker of nonclassical monocyte development, nor did it examine earlier progenitors for this effect. To test whether TREML4 faithfully reports nonclassical monocyte development, we first reconfirmed TREML4 as a marker of nonclassical monocytes in vivo (Fig. 1 *A*–*G*). Total monocytes were partially reduced in *Nr4a1*$^{-/-}$ (*Nr4a1*^{KO}) mice (Fig.1 *A* and *B*) as expected, and both TREML4 and CD11c were selectively induced in Ly6C^{lo} monocytes (Fig. 1 *C*–*G*). Importantly, CD11c and TREML4 expression on monocytes was not observed in *Nr4a1*^{KO} mice. Next, we examined nonclassical monocyte development from earlier progenitors using the OP9 cell line expressing the Notch ligand DLL1 (36). OP9 cells expressing DLL1 (OP9-DLL1) have previously been used to examine the impact of Notch signaling on development of T cells (37) and dendritic cells (38). Purified MDPs from wild-type (WT) mice were cultured on OP9 or OP1-DLL1 cells for 2 d and examined for expression of Ly6C, CC11c, and TREML4 (Fig. 1 *H*–*K*). MDPs cultured on original OP9 cells retained Ly6C expression and did not induce either CD11c or TREML4. By contrast, ~40% of MDPs cultured on OP9-DLL1 cells lost Ly6C expression and induced both CD11c and TREML4. These results suggest that Notch signaling in monocyte progenitors robustly induces nonclassical monocyte development in vitro.

Identification of Nonclassical Monocyte Transcriptional Regulators. We next examined the acute impact of Notch signaling on immediate progenitors of nonclassical monocytes (Fig. 2 *A* and *B*). Purified cMoPs and Ly6C^{hi} monocytes were cultured on OP9 or OP9-DLL1 cells for 6 h and analyzed by RNA-seq. In Ly6C^{hi} monocytes, *Hes1* was the gene most highly induced by DLL1 (Fig. 2*A*) and was induced in cMoPs as well. *Itgax* (encoding CD11c) was among the top 20 most highly DLL1-induced genes (Fig. 2*A*), and *TREML4* was also induced in Ly6C^{hi} monocytes by DLL1 stimulation (Fig. 2*B*). HES1 is a transcriptional repressor (39) known to be induced downstream of Notch signaling (40). We expressed the constitutively active NICD or HES1 into monocyte progenitors by retroviral transduction to compare their respective capacities to drive development of Ly6C^{lo} monocytes (Fig. 2 *C* and *D*). Expression of NICD into progenitors induced development of Ly6C^{lo} TREML4^{+} CD11c^{+} cells in ~60% of the population, similar to the effects of coculture with OP9-DLL1 cells (Fig. 2 *C*–*F*). By contrast, the expression of HES1 failed to induce such a population. HES1 failed to induce any expression of CD11c or loss of Ly6C, but induced TREML4 in approximately 20% of cells (*SI Appendix*, Fig. S1). These results suggest that factors other than HES1 may be required for development of Ly6C^{lo} monocytes.

We compared the expression of transcription factors between MDPs, cMOPs and Ly6C^{hi} and Ly6C^{lo} monocytes (Fig. 2*G*). In agreement with previous studies, we found that *Nr4a1* (30) and *Cebpb* (29), were both more highly expressed in Ly6C^{lo} monocytes than in Ly6C^{hi} monocytes or progenitors. In addition, we also noted interesting expression patterns for *Bcl6*, *Irf2*, and *Ikzf3* (which encodes AIOLOS). *Bcl6* and *Ikzf3* were both highly induced in Ly6C^{lo} monocytes compared with Ly6C^{hi} monocytes. *Irf2* was expressed more highly in Ly6C^{hi} monocytes compared with progenitors, but was increased further in Ly6C^{lo} monocytes. The roles of *Bcl6*, *Ikzf3*, and *Irf2* in Ly6C^{lo} monocyte development have not been examined.

BCL6 Expression in Myeloid Progenitors Is Required for Nonclassical Monocytes. We recently reported that conditional deletion of *Bcl6* under control of *Csf1r*^{Cre} allowed development of cDC1s (41). *Csf1r* is also expressed in monocyte progenitors such as MDPs (20) and GMPs (42). Therefore, we asked whether conditional deletion of *Bcl6* by *Csf1r*^{Cre} altered Ly6C^{lo} monocyte development (Fig. 3). Ly6C^{hi} monocytes developed and were increased in number in blood in *Bcl6*$^{fl/fl}$ × *Csf1r*^{Cre} (*Bcl6*^{cKO}) mice (Fig. 3 *A* and *B*). In contrast, Ly6C^{lo} monocytes in blood were completely absent in *Bcl6*^{cKO} mice, but not in *Bcl6*$^{fl/fl}$ (*Bcl6*^{flox}) mice (Fig. 3 *C* and *D* and *SI Appendix*, Fig. S2). B cells and neutrophils were present in normal numbers in blood in *Bcl6*^{cKO} mice (Fig. 3 *E*–*H*), indicating that the loss of Ly6C^{lo} monocytes was specific. Likewise, Ly6C^{lo} monocytes in BM were completely absent in *Bcl6*^{cKO} mice (Fig. 3 *I* and *J*), while Ly6C^{hi} monocytes in BM were normal (Fig. 3*K*). Of interest, cMoPs and MDPs showed a statistically significant numerical increase of approximately 50% in *Bcl6*^{cKO} mice (Fig. 3 *L* and *M*).

IRF2 Is a Cell-Intrinsic Requirement for Nonclassical Monocytes. *Irf2*$^{-/-}$ mice were reported to have reduced Lyc6C^{lo} monocytes in the setting of infection by West Nile virus, but the homeostatic role of IRF2 in development was not examined (43). First, we observed that naïve *Irf2*$^{-/-}$ (*Irf2*^{KO}) mice had normal numbers of blood Ly6C^{hi} monocytes, but had severely reduced blood Ly6C^{lo} monocytes when compared to *Irf2*$^{+/-}$ (*Irf2*^{het}) mice (Fig. 4 *A*–*D*). In comparison, we observed no difference in blood Ly6C^{lo} monocytes between WT and *Irf2*^{het} mice (*SI Appendix*, Fig. S2). We confirmed that *Irf2*^{KO} mice have reduced B cell numbers in blood but no significant difference in neutrophils (Fig. 4 *E*–*H*), validating previous reports of a B cell defect in *Irf2*^{KO} mice (44). Likewise, BM Ly6C^{lo} monocytes were completely absent in *Irf2*^{KO} mice (Fig. 4 *I* and *J*), while BM Ly6C^{hi} monocytes were modestly increased (Fig. 4*K*). A slight increase in the number of cMoPs, but not MDPs, was observed in *Irf2*^{KO} mice compared with control mice (Fig. 4 *L* and *M*).

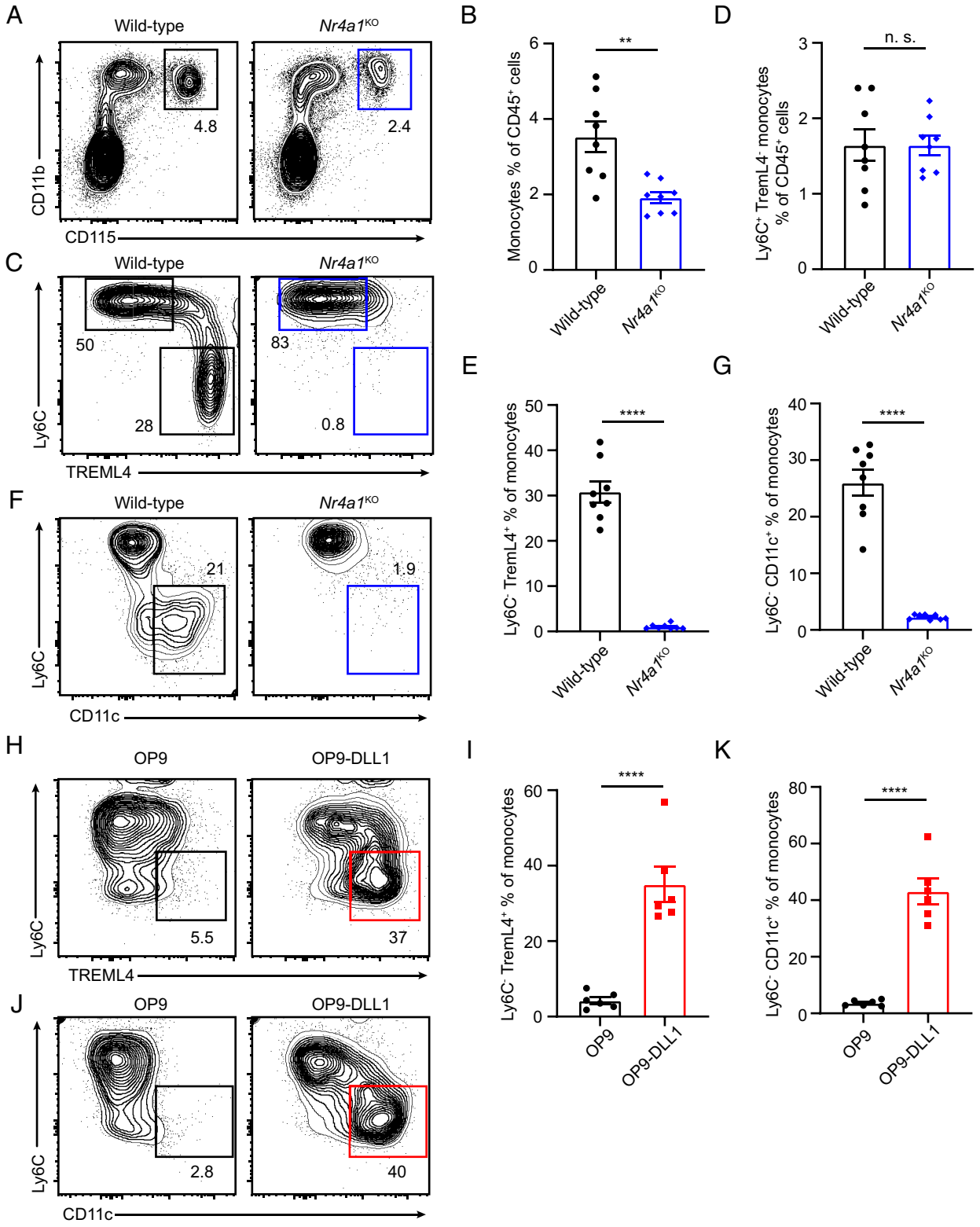

Fig. 1. Notch stimulation induces Ly6C$^-$ TREML4$^+$ CD11c$^+$ nonclassical monocytes. (*A*) Peripheral blood was analyzed from wild-type or *Nr4a1*$^{-/-}$ (*Nr4a1*^{KO}) mice. Shown analysis is pregated on CD45$^+$ single cells. (*B*) Total monocytes (gated as CD45$^+$ CD11b$^+$ CD115$^+$ as in *A*) are shown as a fraction of CD45$^+$ single cells. (*C*) Peripheral blood was analyzed from wild-type or *Nr4a1*^{KO} mice. Shown analysis is pregated on CD45$^+$ CD11b$^+$ CD115$^+$ single cells. (*D*) Ly6C^{hi} classical monocytes (gated as Ly6C$^+$ TREML4$^-$ CD45$^+$ CD11b$^+$ CD115$^+$) are shown as a fraction of CD45$^+$ single cells. (*E*) Ly6C$^-$ TREML4$^+$ cells are shown as a fraction of CD45$^+$ CD11b$^+$ CD115$^+$ cells. (*F*) Peripheral blood was analyzed from wild-type or *Nr4a1*^{KO} mice. Shown analysis is pregated on CD45$^+$ CD11b$^+$ CD115$^+$ single cells. (*G*) Ly6C$^-$ CD11c$^+$ cells are shown as a fraction of CD45$^+$ CD11b$^+$ CD115$^+$ cells. (*H*) MDPs were sorted as Lin$^-$ CD45$^+$ CD115$^+$ CD117$^+$ CD135$^+$ and cocultured with OP9 or OP9-DLL1 stromal cells in SCF, IL-3, and IL-6 for 2 days. Shown is FACS analysis of CD11b$^+$ CD115$^+$ MerTK^{lo} CD64^{lo} cells. (*I*) Ly6C$^-$ TREML4$^+$ cells are shown as a fraction of cultured monocytes (gated as CD11b$^+$ CD115$^+$ MerTK^{lo} CD64^{lo}). (*J*) MDPs were sorted as Lin$^-$ CD45$^+$ CD115$^+$ CD117$^+$ CD135$^+$ and cocultured with OP9 or OP9-DLL1 stromal cells in SCF, IL-3, and IL-6 for 2 days. Shown is FACS analysis of CD11b$^+$ CD115$^+$ MerTK^{lo} CD64^{lo} cells. (*K*) Ly6C$^-$ CD11c$^+$ cells are shown as a fraction of cultured monocytes (gated as CD11b$^+$ CD115$^+$ MerTK^{lo} CD64^{lo}). Bars represent average values ± SEM. $^{**}P < 0.01$, $^{****}P < 0.0001$, n.s. not significant (Student's *t* test).

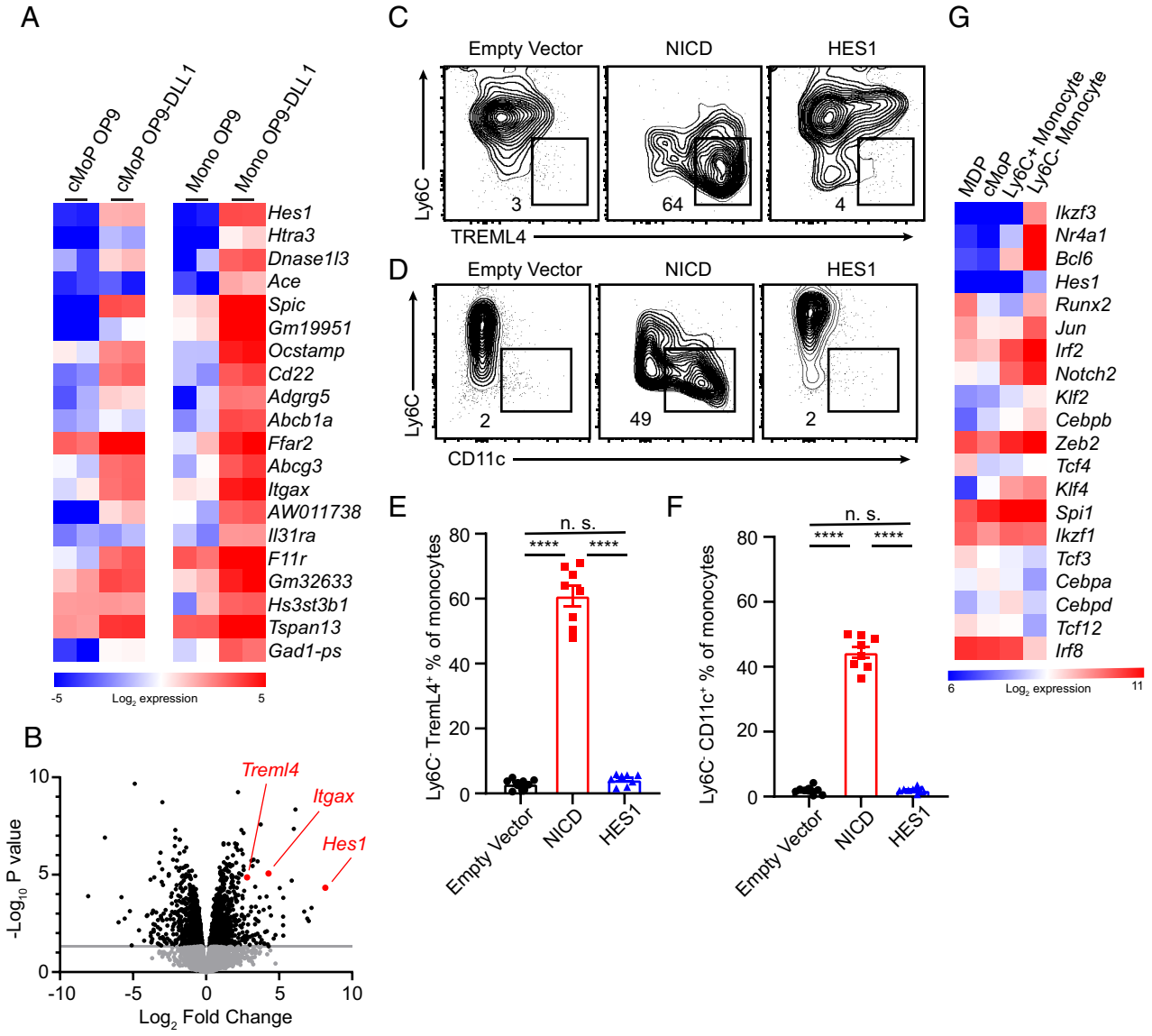

Fig. 2. Characterization of differentially expressed transcription factors in nonclassical monocytes. (*A*) cMoPs (sorted as Lin$^-$ CD45$^+$ CD115$^+$ CD117$^+$ CD135$^-$) and Ly6C^{hi} monocytes (sorted as Lin$^-$ CD45$^+$ CD115$^+$ CD117$^-$ CD135$^-$ Ly6C$^+$ TremL4$^-$) were isolated from bone marrow and cocultured with OP9 or OP9-DLL1 stromal cells in SCF, IL-3, and IL-6 for 6 h before isolation and bulk RNA sequencing. Shown are 20 genes with the greatest fold increase in OP9-DLL1-cocultured Ly6C^{hi} monocytes relative to OP9-cocultured Ly6C^{hi} monocytes among significantly differentially expressed genes (Benjamini–Hochberg adjusted *P*-value < 0.05). (*B*) Volcano plot comparing gene expression in OP9-DLL1-cocultured Ly6C^{hi} monocytes to gene expression in OP9-cocultured Ly6C^{hi} monocytes. (*C* and *D*) Lin$^-$ (CD3ε, CD19, CD105, Ly6G, Ter119) CD117$^+$ progenitor cells were sorted and transduced with plasmids expressing a GFP reporter and either no gene (Empty Vector), the intracellular domain of *Notch2* (NICD), or *Hes1* (HES1). Cells were cultured in SCF, IL-3, and IL-6 for 2 d, then subjected to FACS analysis. Shown populations are pregated on CD11b$^+$ CD115$^+$ MerTK^{lo} CD64^{lo} single cells. (*E* and *F*) Ly6C$^-$ TREML4$^+$ or Ly6C$^-$ CD11c$^+$ cells, respectively, are shown as a fraction of GFP$^+$ CD11b$^+$ CD115$^+$ MerTK^{lo} CD64^{lo} cells. (*G*) Gene expression microarray analysis of MDPs, cMoPs, Ly6C^{hi} monocytes, and Ly6C^{lo} monocytes sorted from bone marrow. Shown are select transcription factors known to influence myeloid development. Bars represent average values ± SEM. ****P < 0.0001, n.s. not significant (Student's *t* test).

Germline-deficient *Irf2*^{KO} mice develop a progressive CD8 T cell–dependent ulcerative dermatitis starting at approximately 8 wk of age which does not occur in *Irf2*^{KO} BM chimeras (45). Since ulcerative dermatitis could conceivably alter Ly6C^{lo} monocyte numbers, we generated BM chimeras using WT and *Irf2*^{KO} BM to test for a cell-intrinsic role for IRF2 in Ly6C^{lo} monocyte development (Fig. 5 and *SI Appendix*, Fig. S3). First, Ly6C^{lo} monocytes developed in WT>WT BM chimeras in spleen, BM, and blood, as expected (Fig. 5 *A*–*F*). In contrast, *Irf2*^{KO}>WT chimeras generated Ly6C^{hi} monocytes, but were completely devoid of Ly6C^{lo} monocytes, indicating a hematopoietic-intrinsic requirement for IRF2. In addition, we also examined mixed BM chimeras (*SI Appendix*, Fig. S3). Since *Irf2*^{KO} BM is poorly competitive with WT BM in mixed chimeras (46), we generated chimeras using a 10:90 ratio of WT to *Irf2*^{KO} BM (*SI Appendix*, Fig. S3). In these mixed chimeras, *Irf2*^{KO} BM was capable of producing MDPs, cMoPs, and Ly6C^{hi} monocytes, but not Ly6C^{lo} monocytes. In contrast, WT BM gave rise to all cell types. In summary, *Irf2* is required in a cell-intrinsic manner in the transition from Ly6C^{hi} monocytes to Ly6C^{lo} monocytes.

Ikzf3 encodes for AIOLOS, a transcription factor which interacts with IKAROS to regulate B development (47, 48) and T cell function (49). As *Ikzf3* is strongly up-regulated in Ly6C^{lo} monocytes relative to Ly6C^{hi} monocytes (Fig. 2*G*), we evaluated *Ikzf3*$^{-/-}$ (*Ikzf3*^{KO}) mice for development of Ly6C^{lo} monocytes. However, we found no significant difference in Ly6C^{lo} monocytes in either the blood (*SI Appendix*, Fig. S4 *A* and *B*) or BM (*SI Appendix*, Fig. S4 *C* and *D*) of *Izkf3*^{KO} mice relative to WT controls.

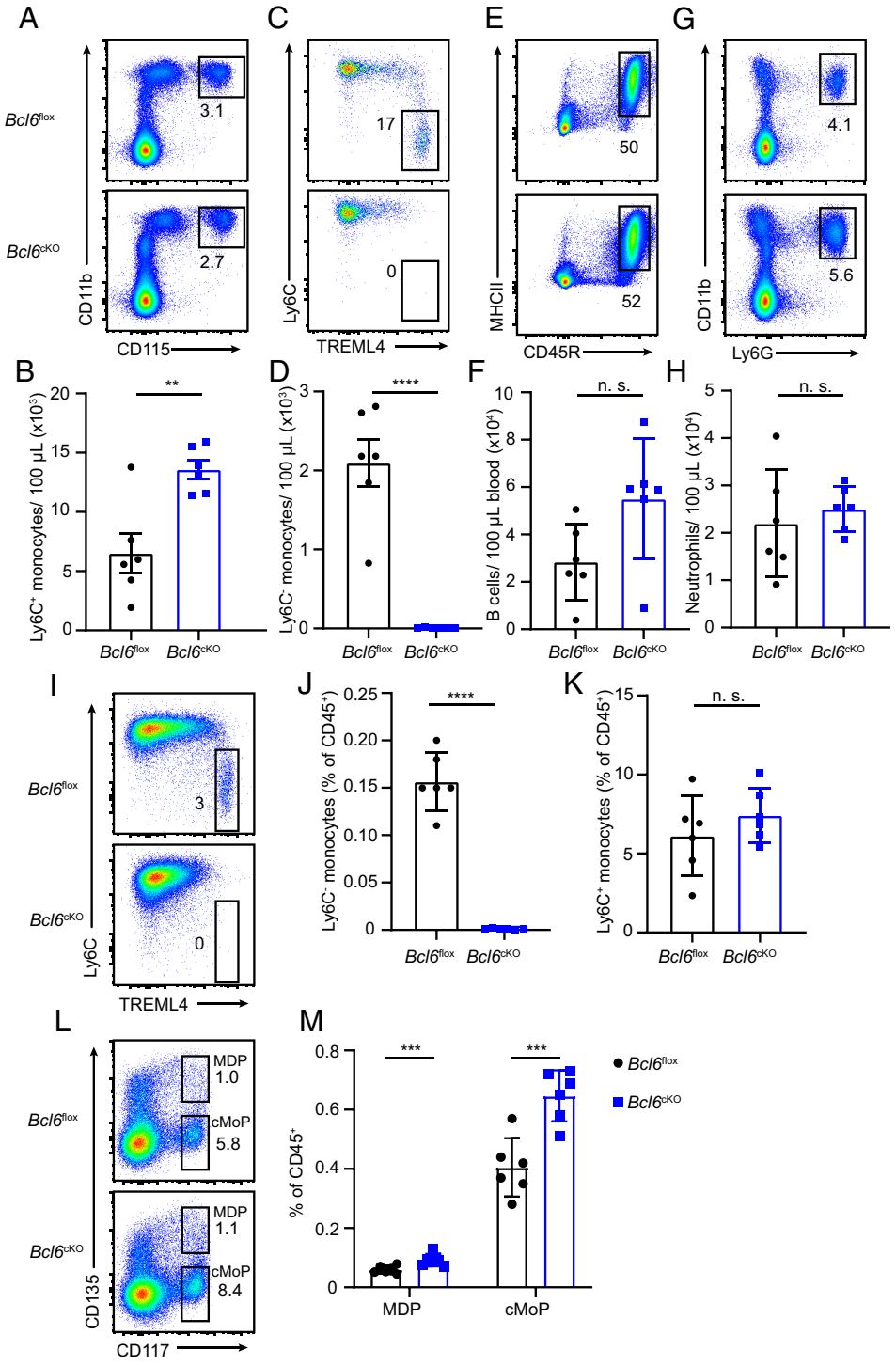

Fig. 3. BCL6 is required for nonclassical monocytes. (*A*) Peripheral blood was analyzed from *Bcl6*$^{flox/flox}$ (*Bcl6*^{flox}) or *Bcl6*$^{flox/flox}$ *Csf1r-cre*$^{+}$ (*Bcl6*^{cKO}) mice for total monocytes. Shown analysis is pregated on CD45^{+} single cells. (*B*) Quantification of Ly6C^{hi} classical monocytes (gated as Ly6C^{+} TREML4^{-} CD11b^{+} CD115^{+} CD45^{+} single cells) per 100 µL peripheral blood. (*C*) Peripheral blood was analyzed as in *A* for Ly6C^{lo} monocytes. Shown analysis is pregated on CD11b^{+} CD115^{+} CD45^{+} single cells. (*D*) Quantification of Ly6C^{lo} nonclassical monocytes (gated as Ly6C^{-} TREML4^{+} CD11b^{+} CD115^{+} CD45^{+} single cells) per 100 µL peripheral blood. (*E*) Peripheral blood was analyzed as in *A* for peripheral B cells. Shown analysis is pregated on CD45^{+} single cells. (*F*) Quantification of peripheral B cells (gated as CD45R^{+} MHCII^{+} CD45^{+} single cells) per 100 µL peripheral blood. (*G*) Peripheral blood was analyzed as in *A* for neutrophils. Shown analysis is pregated on CD45^{+} single cells. (*H*) Quantification of neutrophils (gated as CD11b^{+} Ly6G^{+} CD45^{+} single cells) per 100 µL peripheral blood. (*I*) Bone marrow was analyzed from *Bcl6*^{flox} or *Bcl6*^{cKO} mice for Ly6C^{lo} monocytes. Shown analysis is pregated on Lin^{-} (CD3ε, CD19, CD105, Ly6G, Ter119) CD45^{+} CD115^{+} CD117^{-} CD135^{-} single cells. (*J* and *K*) Quantification of Ly6C^{lo} monocytes (gated as Lin^{-} CD45^{+} CD115^{+} CD117^{-} CD135^{-} Ly6C^{-} TREML4^{+}) or Ly6C^{hi} monocytes (gated as Lin^{-} CD45^{+} CD115^{+} CD117^{-} CD135^{-} Ly6C^{+} TREML4^{-}) as a function of total bone marrow CD45^{+} cells. (*L*) Bone marrow was analyzed as in *I* for MDPs and cMoPs. Shown analysis is pregated on Lin^{-} CD45^{+} CD115^{+} single cells. (*M*) Quantification of MDPs (gated as Lin^{-} CD45^{+} CD115^{+} CD117^{+} CD135^{+}) or cMoPs (gated as Lin^{-} CD45^{+} CD115^{+} CD117^{+} CD135^{-}) as a function of total bone marrow CD45^{+} cells. Bars represent average values ± SEM. $^{**}P < 0.01$, $^{***}P < 0.001$, $^{****}P < 0.0001$, n.s. not significant (Student's *t* test).

Differing Hierarchy of Actions for Transcription Factors in Ly6C^{lo} Monocytes. Our results show that in addition to NUR77, BCL6 and IRF2 are also required for Ly6C^{lo} monocyte development in vivo. We sought to determine whether these transcription factors were also required in vitro for OP9-DLL1-mediated development of Ly6C^{lo} monocytes. To do so, we cocultured MDPs

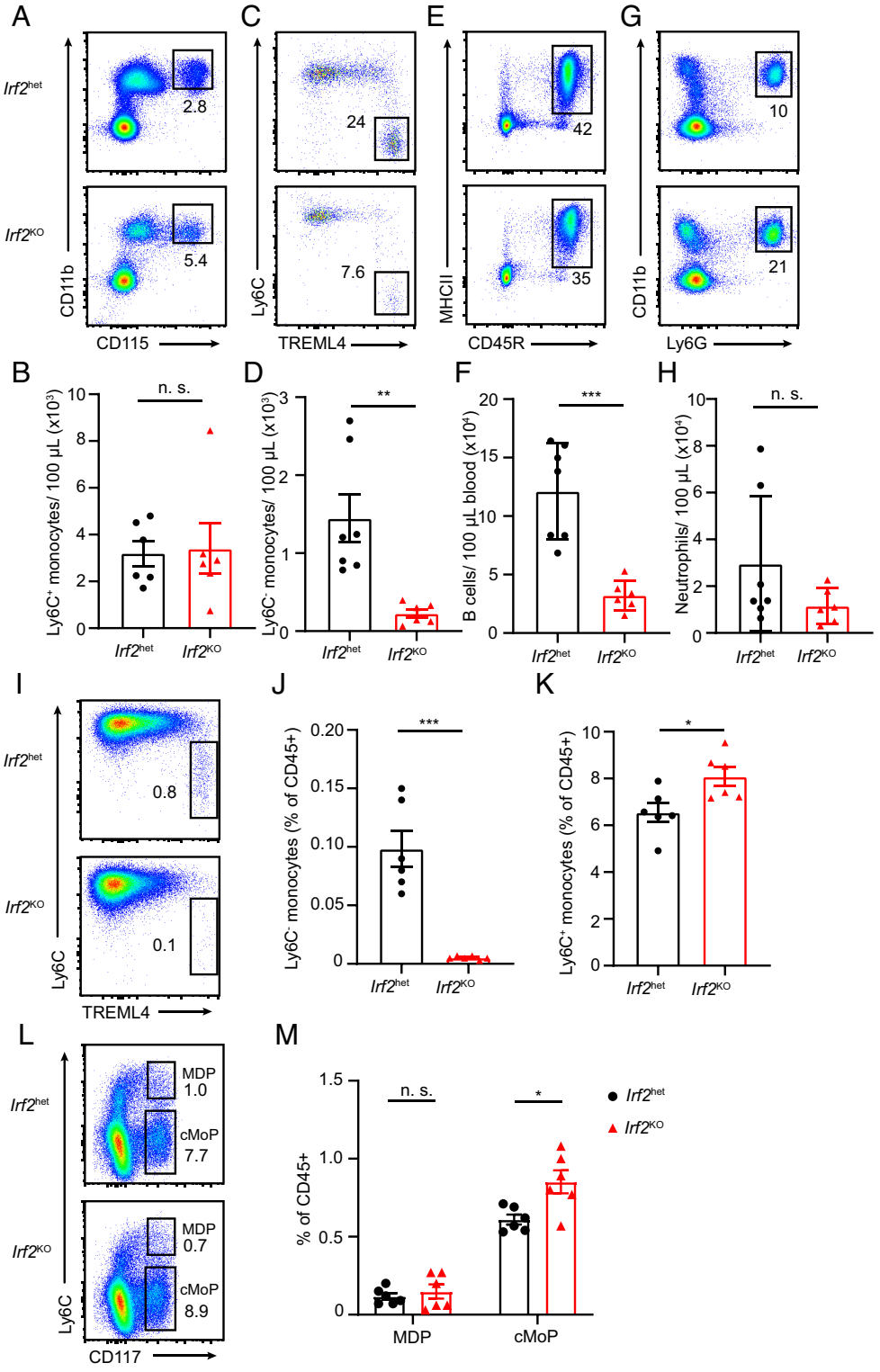

Fig. 4. IRF2 is required for nonclassical monocytes. (*A*) Peripheral blood was analyzed from *Irf2*$^{+/-}$ (*Irf2*^{het}) or *Irf2*$^{-/-}$ (*Irf2*^{KO}) mice for total monocytes. Shown analysis is pregated on CD45$^+$ single cells. (*B*) Quantification of Ly6C^{hi} classical monocytes (gated as Ly6C$^+$ TREML4$^-$ CD11b$^+$ CD115$^+$ CD45$^+$ single cells) per 100 µL peripheral blood. (*C*) Peripheral blood was analyzed as in *A* for Ly6C^{lo} monocytes. Shown analysis is pregated on CD11b$^+$ CD115$^+$ CD45$^+$ single cells. (*D*) Quantification of Ly6C^{lo} nonclassical monocytes (gated as Ly6C$^-$ TREML4$^+$ CD11b$^+$ CD115$^+$ CD45$^+$ single cells) per 100 µL peripheral blood. (*E*) Peripheral blood was analyzed as in *A* for peripheral B cells. Shown analysis is pregated on CD45$^+$ single cells. (*F*) Quantification of peripheral B cells (gated as CD45R$^+$ MHCII$^+$ CD45$^+$ single cells) per 100 µL peripheral blood. (*G*) Peripheral blood was analyzed as in *A* for neutrophils. Shown analysis is pregated on CD45$^+$ single cells. (*H*) Quantification of neutrophils (gated as CD11b$^+$ Ly6G$^+$ CD45$^+$ single cells) per 100 µL peripheral blood. (*I*) Bone marrow was analyzed from *Irf2*^{het} or *Irf2*^{KO} mice for Ly6C^{lo} monocytes. Shown analysis is pregated on Lin$^-$ (CD3ε, CD19, CD105, Ly6G, Ter119) CD45$^+$ CD115$^+$ CD117$^-$ CD135$^-$ single cells. (*J* and *K*) Quantification of Ly6C^{lo} monocytes (gated as Lin$^-$ CD45$^+$ CD115$^+$ CD117$^-$ CD135$^-$ Ly6C$^-$ TREML4$^+$) or Ly6C^{hi} monocytes (gated as Lin$^-$ CD45$^+$ CD115$^+$ CD117$^-$ CD135$^-$ Ly6C$^+$ TREML4$^-$) as a function of total bone marrow CD45$^+$ cells. (*L*) Bone marrow was analyzed as in *I* for MDPs and cMoPs. Shown analysis is pregated on Lin$^-$ CD45$^+$ CD115$^+$ single cells. (*M*) Quantification of MDPs (gated as Lin$^-$ CD45$^+$ CD115$^+$ CD117$^+$ CD135$^+$) or cMoPs (gated as Lin$^-$ CD45$^+$ CD115$^+$ CD117$^+$ CD135$^-$) as a function of total bone marrow CD45$^+$ cells. Bars represent average values ± SEM. *P < 0.05, **P < 0.01, ***P < 0.001, n.s. not significant (Student's t test).

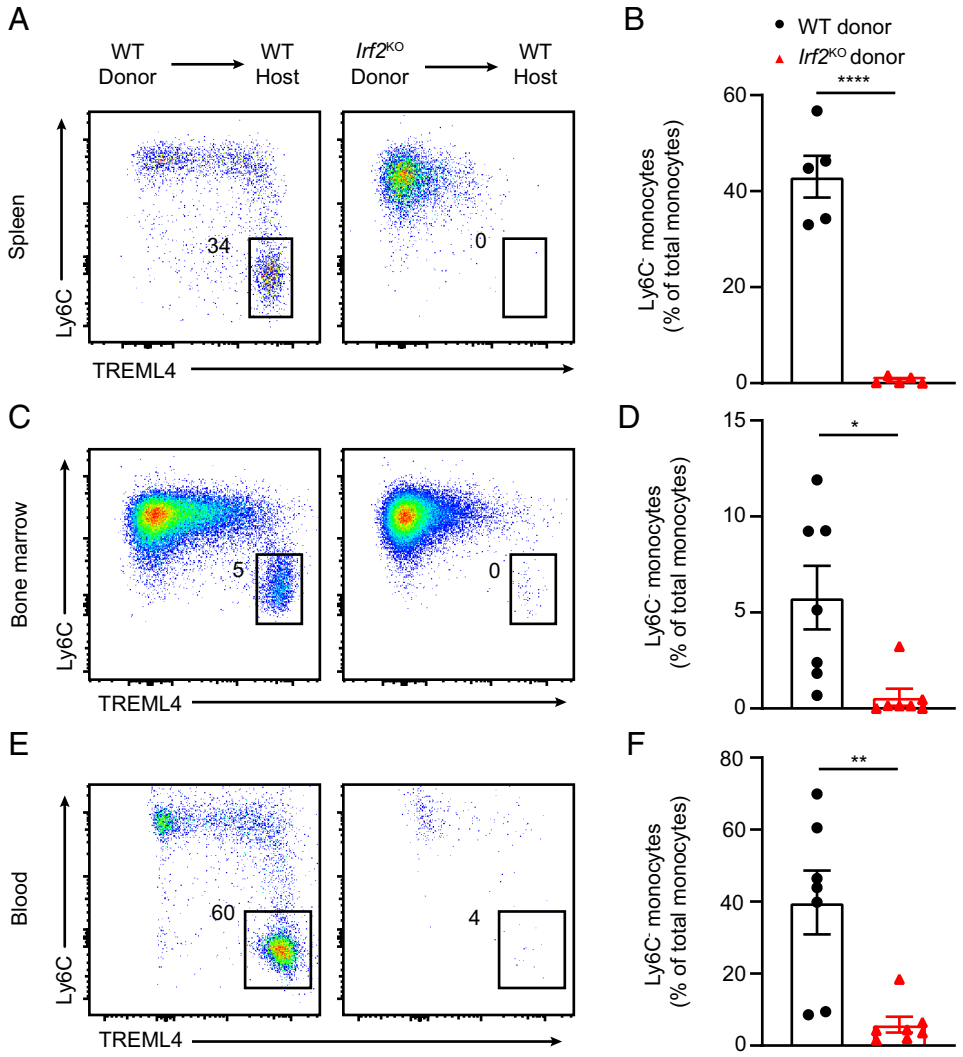

Fig. 5. The requirement for IRF2 in nonclassical monocytes is cell-intrinsic. (*A*) CD45.1-expressing wild-type mice were lethally irradiated and injected i.v. with congenically marked CD45.2$^+$ wild-type or *Irf2*^{KO} bulk bone marrow. Spleen was analyzed 8 wk later via FACS for Ly6C^{lo} monocytes. Shown analysis is pregated on CD45.2$^+$ CD11b$^+$ CD115$^+$ cells. (*B*) Quantification of spleen Ly6C^{lo} monocytes (gated as CD45.2$^+$ Ly6C$^-$ TREML4$^+$ CD11b$^+$ CD115$^+$) as a function of total monocytes (gated as CD45.2$^+$ CD11b$^+$ CD115$^+$). (*C*) Bone marrow chimeras were set up as in *A* and bone marrow was analyzed 8 wk later via FACS for Ly6C^{lo} monocytes. Shown analysis is pregated on CD45.2$^+$ Lin$^-$ (CD3ε, CD19, CD105, Ly6G, Ter119) CD115$^+$ CD117$^-$ CD135$^-$. (*D*) Quantification of bone marrow Ly6C^{lo} monocytes (gated as CD45.2$^+$ Ly6C$^-$ TREML4$^+$ Lin$^-$ CD115$^+$ CD117$^-$ CD135$^-$) as a function of total monocytes (gated as CD45.2$^+$ Lin$^-$ CD115$^+$ CD117$^-$ CD135$^-$). (*E*) Bone marrow chimeras were set up as in *A* and peripheral blood was analyzed 8 wk later via FACS for Ly6C^{lo} monocytes. Shown analysis is pregated on CD45.2$^+$ CD11b$^+$ CD115$^+$ single cells. (*F*) Quantification of peripheral blood Ly6C^{lo} monocytes (gated as CD45.2$^+$ Ly6C$^-$ TREML4$^+$ CD11b$^+$ CD115$^+$) as a function of total monocytes (gated as CD45.2$^+$ CD11b$^+$ CD115$^+$). Bars represent average values ± SEM. *P < 0.05, **P < 0.01, ****P < 0.0001 (Student's t test).

of the relevant genotypes with either OP9 or OP9-DLL1 cells for 2 d and examined cells for expression of Ly6C and TREML4. We found that MDPs from *Nr4a1*^{KO} mice generated Ly6C$^-$ TREML4$^+$ cells at rates similar to WT MDPs in OP9-DLL1 cell coculture (Fig. 6 *A* and *B*). Similarly, we found no significant difference in the generation of Ly6C$^-$ TREML4$^+$ cells from *Bcl6*^{flox} or *Bcl6*^{cKO} MDPs (Fig. 6 *C* and *D* and *SI Appendix*, Fig. S5). In contrast, Ly6C$^-$ TREML4$^+$ cells failed to develop from *Irf2*^{KO} MDPs and were reduced in number from *Irf2*^{het} MDPs (Fig. 6 *E* and *F* and *SI Appendix*, Fig. S5). However, we observed that Ly6C$^+$ TREML4$^+$ cells developed from both *Irf2*^{het} and *Irf2*^{KO} MDPs in OP9-DLL1 coculture, despite developing from neither in OP9 coculture (Fig. 6 *E* and *G*). This suggests that IRF2 is required to finish development to a nonclassical monocyte–resembling Ly6C$^-$ TREML4$^+$ state, though it is not required for the Notch-mediated initiation of this developmental pathway. In conclusion, NUR77 and BCL6 are required for nonclassical monocyte development in vivo but not in vitro, while IRF2 is required for nonclassical monocytes both in vivo and in vitro.

To determine early effector targets of NUR77, BCL6, and IRF2, we conducted RNA-Seq of BM Ly6C^{hi} monocytes derived from WT, *Nr4a1*^{KO}, *Bcl6*^{cKO}, and *Irf2*^{KO} mice (Fig. 7*A*). In *Nr4a1*^{KO} mice, we observed loss of *Nr4a1* expression, but expression of *Bcl6*, *Irf2*, and other transcription factors involved in myeloid development were not altered (Fig. 7*B* and *SI Appendix*, Fig. S6). Similarly, *Bcl6*^{cKO} Ly6C^{hi} monocytes had no change in expression of *Nr4a1*, *Irf2*, or other important transcription factors (Fig. 7*C* and *SI Appendix*, Fig. S6). We did observe an increase in *Bcl6* mRNA expression, which is attributable to a lack of functional BCL6 protein causing a failure of autorepression at the *Bcl6* locus (41, 50, 51). However, *Irf2*^{KO} Ly6C^{hi} monocytes had significant reduction in *Bcl6* and *Nr4a1* expression (Fig. 7*D*). These combined data suggest that IRF2 may regulate a hierarchy of transcription factors including BCL6 and

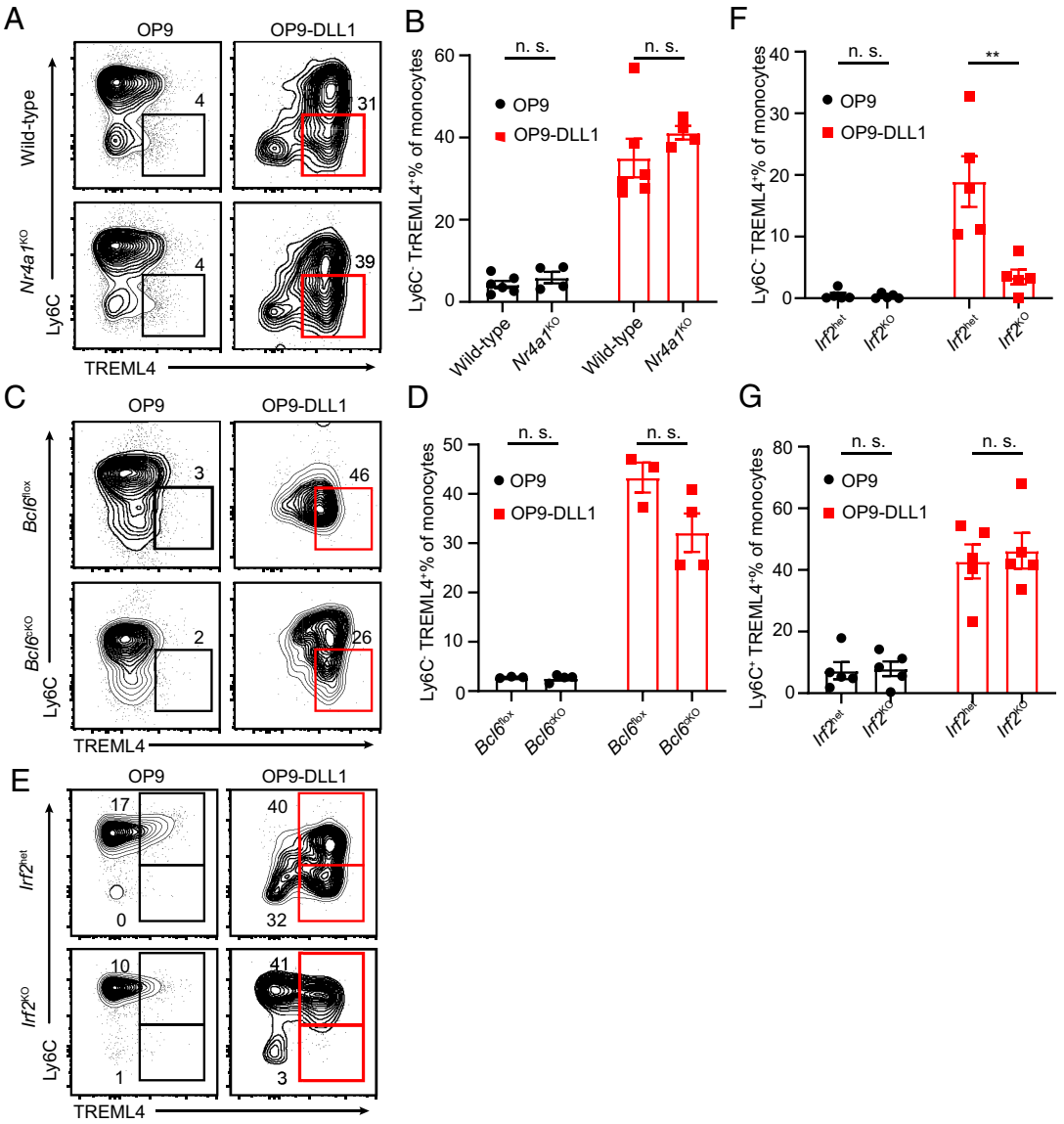

Fig. 6. IRF2 but not NUR77 or BCL6 are required for Notch-induced nonclassical monocyte development. (*A*) Sort-purified wild-type or *Nr4a1*^{KO} MDPs (sorted as Lin$^-$ CD45$^+$ CD115$^+$ CD117$^+$ CD135$^+$) were cocultured with OP9 or OP9-DLL1 stromal cells in SCF, IL-3, and IL-6 for 2 d. Shown is FACS analysis of CD11b$^+$ CD115$^+$ MerTK^{lo} CD64^{lo} cells. (*B*) Ly6C$^-$ TREML4$^+$ cells are shown as a fraction of cultured monocytes (gated as CD11b$^+$ CD115$^+$ MerTK^{lo} CD64^{lo}). (*C*) Sort-purified *Bcl6*^{flox} or *Bcl6*^{cKO} MDPs were cocultured with OP9 or OP9-DLL1 stromal cells in SCF, IL-3, and IL-6 for 2 d. Shown is FACS analysis of CD11b$^+$ CD115$^+$ MerTK^{lo} CD64^{lo} cells. (*D*) Ly6C$^-$ TREML4$^+$ cells are shown as a fraction of cultured monocytes (gated as in *B*). (*E*) Sort-purified *Irf2*^{het} or *Irf2*^{KO} MDPs were cocultured with OP9 or OP9-DLL1 stromal cells in SCF, IL-3, and IL-6 for 2 d. Shown is FACS analysis of CD11b$^+$ CD115$^+$ MerTK^{lo} CD64^{lo} cells. (*F* and *G*) Ly6C$^-$ TREML4$^+$ and Ly6C$^+$ TREML4$^+$ cells, respectively, are shown as a fraction of cultured monocytes (gated as in *B*). Bars represent average values ± SEM. $^{**}P < 0.01$, n.s. not significant (Student's *t* test).

NUR77, which are required ultimately for differentiation of Ly6C^{lo} nonclassical monocytes.

Discussion

Nonclassical monocytes were first recognized in humans as a subset of circulating PBMCs that bind antigen–antibody complexes (3) and express CD16 (4). Nonclassical monocytes were subsequently recognized in mice as a PBMC population expressing CX_3CR1 (12) and later as a Ly6C^{lo} CD11c$^+$ (13) or Ly6C^{lo} TREML4$^+$ (14) PBMC population. The role for nonclassical monocytes in surveillance of vasculature was inferred by their adherent patrolling motion along endothelial surfaces (15, 16) and from their ability to protect tissues from tumor metastasis (17). Despite their clear importance, our understanding of their development remains relatively incomplete. In mice, the transcription factors NUR77 (30) and C/EBPβ (29) are known to be required for Ly6C^{lo} monocytes, and signaling by NOTCH2 has been suggested as a component of their development (35), but these factors have not been confirmed as requirements for nonclassical monocytes in humans. Conversely, mutations in human IKAROS (52) and STAT3 (53) have been associated with loss of nonclassical monocytes, but have not been confirmed mice. It is largely unknown how these various factors function in Ly6C^{lo} monocytes. This study identifies the transcription factors BCL6 and IRF2 as additional requirements for Ly6C^{lo} monocytes.

We initiated this work to reexamine the role of NOTCH2 signaling in Ly6C^{lo} monocyte development. In agreement with previous work (35), we confirm that activation of NOTCH2 signaling induces Ly6C^{lo} monocyte development. We determined the early transcriptional response to NOTCH2 signaling in cMoPs and Ly6C^{hi} monocytes, and identified HES1 as the most highly

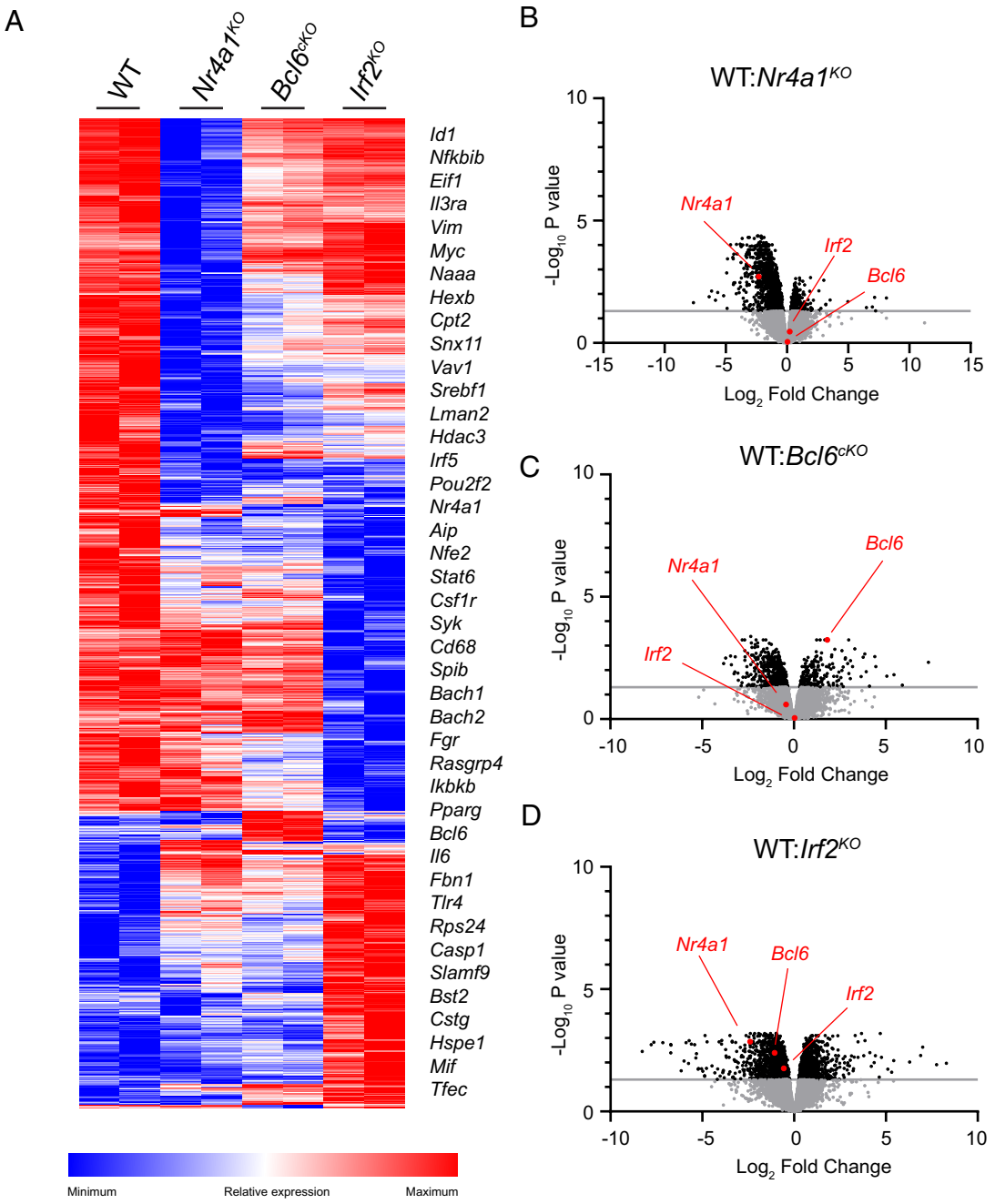

Fig. 7. Loss of IRF2 reduces *Bcl6* and *Nr4a1* expression in Ly6C^{hi} monocytes. (*A*) Ly6C^{hi} monocytes were obtained from WT, *Nr4a1*^{KO} *Bcl6*^{cKO}, and *Irf2*^{KO} BM and subjected to RNA sequencing. Shown is a heat map displaying differentially expressed genes organized by hierarchical clustering. (*B*) Volcano plot comparing gene expression in WT BM Ly6C^{hi} monocytes to gene expression in *Nr4a1*^{KO} BM Ly6C^{hi} monocytes, as determined by RNA-Seq. (*C*) Volcano plot comparing gene expression in WT BM Ly6C^{hi} monocytes to gene expression in *Bcl6*^{cKO} BM Ly6C^{hi} monocytes, as determined by RNA-Seq. (*D*) Volcano plot comparing gene expression in WT BM Ly6C^{hi} monocytes to gene expression in *IRF2*^{KO} BM Ly6C^{hi} monocytes, as determined by RNA-Seq.

induced target. However, our results show that HES1 expression alone could only partially induce the Ly6C^{lo} monocyte transition. In contrast, we found that expression of the NICD fully induced the Ly6C^{lo} monocyte transition. These results suggest that the NICD engages additional targets beyond HES1 during the transition to the Ly6C^{lo} monocyte fate. Further work will be required to fully identify the NICD targets that are responsible for this transition.

Our work has added two additional transcription factors, BCL6 and IRF2, to the small set of factors known as requirements for the Ly6C^{lo} monocyte transition. Previously, NUR77 and C/EBPβ were recognized as being involved in Ly6C^{lo} monocyte development, although their precise function in this process remains obscure. NUR77 was first recognized as being highly expressed in Ly6C^{lo} monocytes (30) based on evaluation of *Nr4a1*^{GFP} reporter mice (54) and was confirmed as a requirement based on analysis of *Nr4a1*$^{-/-}$ mice (55). A role for C/EBPβ was observed in *Cebpb*$^{-/-}$ mice, in which Ly6C^{lo} monocytes are absent (29, 33). The function of C/EBPβ in sustaining Ly6C^{lo} monocytes is currently unclear, but C/EBPβ may support MCSFR expression (33) or induce *Nr4a1* expression (29). However, these hypotheses have not been directly tested.

Here, we demonstrate cell-intrinsic requirements for BCL6 and IRF2 in Ly6C^{lo} monocyte development. BCL6 is a transcriptional

repressor known to be required for development of germinal center B cells (56) and T follicular helper cells (57), but the targets of BCL6 in these cells remain undefined. IRF2 limits the expression of genes induced by IFNAR signaling (44, 45). *Irf2*$^{-/-}$ mice show defects in natural killer cell maturation (58) and hematopoietic stem cell maintenance (59), and increased development of basophils (60). However, the molecular targets mediating these effects are currently unclear. The current challenge for understanding the functions of BCL6 and IRF2 lies in determining the precise transcriptional targets of these factors.

Currently, no model unifies the requirements of NOTCH2, NUR77, and C/EBPβ to explain processes governing the development of nonclassical monocytes. Our findings of BCL6 and IRF2 as additional requirements only increase the complexity of this problem. Nonetheless, knowledge of these additional factors will be essential in determining how nonclassical monocytes develop. Previous work suggests mechanisms by which these factors may interact. BCL6 has been proposed as a necessary modulator of Notch signaling in mouse neural stem/progenitor cells and in *Xenopus* lateral plate mesoderm, repressing select Notch targets while other Notch targets are activated (61, 62). Recently, *Irf2*$^{-/-}$ tumor-infiltrating CD8^{+} T cells were predicted to have less BCL6 activity based on Ingenuity Pathway Analysis (63). Further work will be necessary to understand how these transcription factors interact to drive nonclassical monocyte development. Understanding of the transcriptional cascade driving nonclassical monocyte development will inform studies of these cells' function and may help in developing therapeutics based around nonclassical monocytes.

Materials and Methods

Mice. WT C57BL6/J, *Bcl6*^{flox} [B6.129S(FVB)-*Bcl6*$^{tm1.1Dent}$/J], *Csf1r*^{Cre} [C57BL/6-Tg(Csf1r-cre)1Mnz/J], *Nr4a1*$^{-/-}$ (B6;129S2-Nr4a1^{tm1Jmi}/J), and *Irf2*$^{-/-}$ (B6.129S2-Irf2^{tm1Mak}/J) mice were obtained from the Jackson Laboratory. *Ikzf3*$^{-/-}$ mice were a gift of Katia Georgopoulos (Harvard Medical School). B6.SJL (B6.SJL-*Ptprc*^{a} *Pepc*^{b}/BoyJ) mice were obtained from Charles River. All mice were maintained on the C57BL/6 background in the Washington University in St. Louis School of Medicine specific pathogen-free animal facility following institutional guidelines with protocols approved by Animal Studies Committee at Washington University in St. Louis. Experiments were performed with mice between 6 and 10 wk of age unless otherwise noted.

Flow Cytometry, Sorting, and Cell Culture. Peripheral blood was collected via submandibular vein bleed using a 5-mm lancet (Fisher Scientific) into EDTA-coated tubes (BD Biosciences). Red blood cells were subsequently lysed in ammonium chloride–potassium bicarbonate (ACK) lysis buffer prior to staining. BM was isolated via crushed hips, femurs, and tibias in phosphate buffered saline (PBS) with 5% fetal bovine serum (FBS) and 2mM EDTA. Cells were passed through a 70-μm filter, and red blood cells were lysed in ACK lysis buffer prior to staining. Splenocytes were collected by mincing spleens, which were then digested for 30 min at 37 °C with stirring in 5 mL complete IMDM (IMDM supplemented with 10% FBS, 1% penicillin–streptomycin solution, 1% sodium pyruvate, 1% MEM nonessential amino acids, 1% L-glutamine, and 55 μM 2-mercaptoethanol) with 250 μg/mL collagenase B (Roche) and 30 U/mL DNAse I (Roche). After digestion, red blood cells were lysed in ACK lysis buffer, and remaining cells were passed through a 70-μm filter to create a single-cell suspension. Cells were stained at 4 °C in PBS with 5% FBS, 2mM EDTA, and Fc block (2.4G2). Lineage depletion was performed with MagniSort™ streptavidin-negative selection bead (Invitrogen) or Mojosort™ streptavidin nanobeads (BioLegend) as needed. Flow cytometry analysis was performed using an Aurora spectral flow cytometer (Cytek). Cell sorting was performed using a FACSAria Fusion flow cytometer (BD Biosciences). Cells were sorted into complete IMDM. After sorting, indicated cells were cultured in complete IMDM supplemented with 5% Flt3L-conditioned media, 5% IL-3-conditioned media, and 5% IL-6-conditioned media for the indicated durations. In indicated experiments, sorted cells were cocultured with either OP9 cells (36) or OP9 cells retrovirally expressing the Notch ligand DLL1 (OP9-DLL1 cells) (37). Data were analyzed using FlowJo software (Tree Star Software).

Antibodies. Biotin-conjugated anti-mouse CD3ε (145-2C11), Brilliant Violet (BV) 421- conjugated anti-mouse CD11b (M1/70), Alexa Fluor (AF) 647-conjugated anti-mouse CD11c (N418), biotin-conjugated anti-mouse CD19 (6D5), PE-Cy7-conjugated CD24 (M1/69), BV711- or allophycocyanin (APC)-Cy7- conjugated anti-mouse CD45.1 (A20), AF488-, BV605-, or PE-Cy7-conjugated anti-mouse CD45.2 (104), AF488- or PE/Dazzle™594- conjugated anti-mouse CD45R (RA3-6B2), BV605-conjugated anti-mouse CD64 (X54-5/7.1), BV711-conjugated anti-mouse CD115 (AFS98), biotin- or PerCP-Cy5.5- conjugated anti-mouse Ly6G (1A8), BV510-conjugated anti-mouse MHC class II I-A/I-E (M5/114.15.2), biotin-conjugated anti-mouse TER-119 (TER-119), and PE-conjugated anti-mouse TREML4 (16E5) were purchased from BioLegend. APC-eFluor780-conjugated anti-mouse CD11c (N418), biotin-conjugated anti-mouse CD105 (MJ7/18), PerCP-eFluor710-conjugated anti-mouse CD172α, APC-conjugated anti-mouse CD317 (eBio927), PE-Cy7-conjugated anti-mouse MerTK (DS5MMER), and Qdot™605-conjugated streptavidin were purchased from Invitrogen. Ultraviolet 395-cojugated anti-mouse CD45R (RA3-6B2), Brilliant Ultraviolet 395-cojugated anti-mouse CD117 (2B8), PE-CF594-conjugated anti-mouse CD135 (A2F10.1), APC-conjugated anti-mouse Ly6C (AL-21), and V500-conjugated anti-mouse MHC class II I-A/I-E (M5/114.15.2) were purchased from BD Biosciences. PerCP-Cy5.5-conjugated anti-mouse CD11b (M1/70) and eFluor450-conjugated anti-mouse CD317 (eBio927) were purchased from eBioscience. PE-Cy7-conjugated anti-mouse CD45.1 and PE-Cy7-conjugated anti-mouse MHC class II I-A/I-E (M5/114.15.2) were purchased from TONBO Biosciences. PerCP-Cy5.5-conjugated anti-mouse CD45.2 (104) was purchased from Fisher Scientific.

RNA-Seq. To explore the effects of Notch stimulation on monocytes, Ly6C^{hi} monocytes or cMoPs were sort purified from BM after lineage depletion (CD3ε, CD19, CD105, Ly6G, TER119) and cultured in complete IMDM supplemented with 5% Flt3L-conditioned media, 5% IL-3-conditioned media, and 5% IL-6-conditioned media and either OP9 or OP9-DLL1 cells for 6 h. To compare differences in WT, *Nr4a1*^{KO}, *Bcl6*^{cKO}, and *Irf2*^{KO} Ly6C^{hi} monocytes, Ly6C^{hi} monocytes were sort purified from BM of each genotype after lineage depletion (CD3ε, CD19, CD105, Ly6G, TER119). In both experiments, RNA was isolated using a NucleoSpin RNA XS kit (Macherey-Nagel) per the manufacturer's protocol. RNA-seq libraries were prepared with 10 μg of total RNA using the SMARTer Ultra Low RNA kit for Illumina Sequencing (Takara-Clontech) per the manufacturer's protocol and sequenced on an Illumina NovaSeq 6000 as paired-end reads extending 150 bases. RNA-seq reads were aligned to mouse reference genome (GRCm38/ mm10) with STAR version 2.7.9a. Gene counts were derived from the number of uniquely aligned unambiguous reads by Subread:featureCount version 2.0.3. All gene counts were then imported into the R/Bioconductor package EdgeR and TMM normalization size factors were calculated to adjust for samples for differences in library size.

Plasmids, Retroviral Packaging, and Overexpression. NICD was amplified from Addgene plasmid #20184 (gift from Raphael Kopan) using primers attattagatctgccaccatggactacaaagacc and attattagatctgcgatccctatgcatacacctg and cloned as a BglII fragment into a murine stem cell virus (MSCV)-based retroviral vector to generate MSCV-IRES-GFP-NICD. HES1 was amplified from Addgene plasmid #17622 (gift from Linzhao Chen) using primers ggaaagatctatgccagctgatataatggagaaa and ggaactcgagctcagttccgccacggtc and cloned as a BglII/XhoI fragment into an MSCV-based retroviral vector to generate MSCV-IRES-GFP-HES1. To package constructs, Platinum-E cells (64) were plated in six-well plates at an approximate density of 10^6 cells per well and incubated overnight. Retroviral plasmid DNA was combined with TransIT-LT1 (Mirus Bio) in Opti-MEM™ (Gibco) and transfected into Platinum-E cells. Cells were incubated overnight, culture media were changed, and the retrovirus-containing supernatant was used 24 h later. Lin^{-} CD117^{+} BM progenitors were sort-purified and transduced with retrovirus-containing supernatant in 2 μg/mL polybrene by spinoculation at 729 × g for 1 h at room temperature. Cell culture media were changed 24 h postspinoculation, and cells were analyzed after another 24 h of culture.

Microarray. Total RNA was extracted from sort-purified BM MDPs, cMoPs, Ly6C^{hi} monocytes, and Ly6C^{lo} monocytes using an RNAqueous-Micro Kit (Ambion). RNA was amplified using the Ovation Pico WTA Sytem (NuGEN) and hybridized to GeneChip Mouse Gene 1.0 ST microarrays (Affymetrix). Data were processed using robust multiarray average summarization and quartile normalization using ArrayStar software, version 5 (DNASTAR). Expression values represent one biological replicate.

BM Chimeras. CD45.1$^+$ mice (B6.SJL-*Ptprc*^{a} *Pepc*^{b}/BoyJ) were lethally irradiated with a dose of 1,050 rads. Mice were injected i.v. 24 h later with either CD45.2$^+$ WT BM, CD45.2$^+$ *Irf2*$^{-/-}$ BM, or a 90:10 mixture of CD45.2$^+$ *Irf2*$^{-/-}$ and CD45.1$^+$ WT BM. Mice were analyzed at least 8 wk later.

Statistics. All statistical analyses were performed using GraphPad Prism software version 8. Unless otherwise noted, Mann–Whitney test was used to determine significant differences between samples. Values are presented as the average ± SEM. $P \leq 0.05$ was considered statistically significant. Heatmaps were generated using Morpheus, https://software.broadinstitute.org/morpheus.

Data, Materials, and Software Availability. RNA-seq data and microarray data are available on the Gene Expression Omnibus (GEO) database with the accession number GSE218504 (65).

ACKNOWLEDGMENTS. We would like to acknowledge Charles Shen and Feiya Ou for assistance and technical advice regarding RNA-Seq. This publication is solely the responsibility of the authors and does not necessarily represent the official view of the NIH. This work was supported by the NIH (R01AI150297, R01CA248919, R01AI162643, and R21AI164142 to K.M.M.)

1. S. Epelman, K. J. Lavine, G. J. Randolph, Origin and functions of tissue macrophages. *Immunity* **41**, 21–35 (2014).
2. P. B. Narasimhan, P. Marcovecchio, A. A. J. Hamers, C. C. Hedrick, Nonclassical monocytes in health and disease. *Annu. Rev. Immunol.* **37**, 439–456 (2019).
3. M. Zembala, W. Uracz, I. Ruggiero, B. Mytar, J. Pryjma, Isolation and functional characteristics of FcR+ and FcR- human monocyte subsets *J. Immunol.* **133**, 1293–1299 (1984).
4. B. Passlick, D. Flieger, H. W. Ziegler-Heitbrock, Identification and characterization of a novel monocyte subpopulation in human peripheral blood. *Blood* **74**, 2527–2534 (1989).
5. H. W. Ziegler-Heitbrock *et al.*, The novel subset of CD14+/CD16+ blood monocytes exhibits features of tissue macrophages. *Eur. J. Immunol.* **23**, 2053–2058 (1993).
6. G. Fingerle *et al.*, The novel subset of CD14+/CD16+ blood monocytes is expanded in sepsis patients. *Blood* **82**, 3170–3176 (1993).
7. W. A. Nockher, L. Bergmann, J. E. Scherberich, Increased soluble CD14 serum levels and altered CD14 expression of peripheral blood monocytes in HIV-infected patients. *Clin. Exp. Immunol.* **98**, 369–374 (1994).
8. W. A. Nockher, J. E. Scherberich, Expanded CD14+ CD16+ monocyte subpopulation in patients with acute and chronic infections undergoing hemodialysis *Infect. Immun.* **66**, 2782–2790 (1998).
9. A. Rivier *et al.*, Blood monocytes of untreated asthmatics exhibit some features of tissue macrophages. *Clin. Exp. Immunol.* **100**, 314–318 (1995).
10. N. Thieblemont, L. Weiss, H. M. Sadeghi, C. Estcourt, N. Haeffner-Cavaillon, CD14lowCD16high: A cytokine-producing monocyte subset which expands during human immunodeficiency virus infection. *Eur. J. Immunol.* **25**, 3418–3424 (1995).
11. S. Jung *et al.*, Analysis of fractalkine receptor CX(3)CR1 function by targeted deletion and green fluorescent protein reporter gene insertion. *Mol. Cell. Biol.* **20**, 4106–4114 (2000).
12. F. Geissmann, S. Jung, D. R. Littman, Blood monocytes consist of two principal subsets with distinct migratory properties. *Immunity* **19**, 71–82 (2003).
13. C. Sunderkötter *et al.*, Subpopulations of mouse blood monocytes differ in maturation stage and inflammatory response. *J. Immunol.* **172**, 4410–4417 (2004).
14. M. A. Ingersoll *et al.*, Comparison of gene expression profiles between human and mouse monocyte subsets. *Blood* **115**, e10–9 (2010).
15. C. Auffray *et al.*, Monitoring of blood vessels and tissues by a population of monocytes with patrolling behavior. *Science* **317**, 666–670 (2007).
16. L. M. Carlin *et al.*, Nr4a1-dependent Ly6C(low) monocytes monitor endothelial cells and orchestrate their disposal. *Cell* **153**, 362–375 (2013).
17. R. N. Hanna *et al.*, Patrolling monocytes control tumor metastasis to the lung. *Science* **350**, 985–990 (2015).
18. P. B. Narasimhan *et al.*, Patrolling monocytes control NK cell expression of activating and stimulatory receptors to curtail lung metastases. *J. Immunol.* **204**, 192–198 (2020).
19. G. D. Thomas *et al.*, Deleting an Nr4a1 super-enhancer subdomain ablates Ly6C(low) monocytes while preserving macrophage gene function. *Immunity* **45**, 975–987 (2016).
20. D. K. Fogg *et al.*, A clonogenic bone marrow progenitor specific for macrophages and dendritic cells. *Science* **311**, 83–87 (2006).
21. C. Varol *et al.*, Monocytes give rise to mucosal, but not splenic, conventional dendritic cells. *J. Exp. Med.* **204**, 171–180 (2007).
22. J. Hettinger *et al.*, Origin of monocytes and macrophages in a committed progenitor. *Nat. Immunol.* **14**, 821–830 (2013).
23. S. Kawamura *et al.*, Identification of a human clonogenic progenitor with strict monocyte differentiation potential: A counterpart of mouse cMoPs. *Immunity* **46**, 835–848.e4 (2017).
24. J. K. Alder *et al.*, Kruppel-like factor 4 is essential for inflammatory monocyte differentiation in vivo. *J. Immunol.* **180**, 5645–5652 (2008).
25. M. W. Feinberg *et al.*, The Kruppel-like factor KLF4 is a critical regulator of monocyte differentiation. *EMBO J.* **26**, 4138–4148 (2007).
26. D. Kurotaki *et al.*, Essential role of the IRF8-KLF4 transcription factor cascade in murine monocyte differentiation. *Blood* **121**, 1839–1849 (2013).
27. E. W. Scott, M. C. Simon, J. Anastasi, H. Singh, Requirement of transcription factor PU.1 in the development of multiple hematopoietic lineages. *Science* **265**, 1573–1577 (1994).
28. S. Yona *et al.*, Fate mapping reveals origins and dynamics of monocytes and tissue macrophages under homeostasis. *Immunity* **38**, 79–91 (2013).
29. A. Mildner *et al.*, Genomic characterization of murine monocytes reveals C/EBPβ transcription factor dependence of Ly6C- cells. *Immunity* **46**, 849–862.e7 (2017).
30. R. N. Hanna *et al.*, The transcription factor NR4A1 (Nur77) controls bone marrow differentiation and the survival of Ly6C- monocytes. *Nat. Immunol.* **12**, 778–785 (2011).
31. R. N. Hanna *et al.*, NR4A1 (Nur77) deletion polarizes macrophages toward an inflammatory phenotype and increases atherosclerosis. *Circ. Res.* **110**, 416–427 (2012).
32. X. Liu *et al.*, Genome-wide analysis identifies NR4A1 as a key mediator of T cell dysfunction. *Nature* **567**, 525–529 (2019).
33. A. Tamura *et al.*, C/EBPbeta is required for survival of Ly6C(-) monocytes. *Blood* **130**, 1809–1818 (2017).
34. A. Tamura *et al.*, Accelerated apoptosis of peripheral blood monocytes in Cebpb-deficient mice. *Biochem. Biophys. Res. Commun.* **464**, 654–658 (2015).
35. J. Gamrekelashvili *et al.*, Regulation of monocyte cell fate by blood vessels mediated by notch signalling. *Nat. Commun.* **7**, 12597 (2016).
36. T. Nakano, H. Kodama, T. Honjo, Generation of lymphohematopoietic cells from embryonic stem cells in culture. *Science* **265**, 1098–1101 (1994).
37. T. M. Schmitt, J. C. Zúñiga-Pflücker, Induction of T cell development from hematopoietic progenitor cells by delta-like-1 in vitro. *Immunity* **17**, 749–756 (2002).
38. M. E. Kirkling *et al.*, Notch signaling facilitates in vitro generation of cross-presenting classical dendritic cells. *Cell Rep.* **23**, 3658–3672.e6 (2018).
39. Y. Sasai, R. Kageyama, Y. Tagawa, R. Shigemoto, S. Nakanishi, Two mammalian helix-loop-helix factors structurally related to Drosophila hairy and Enhancer of split. *Genes Dev.* **6**, 2620–2634 (1992).
40. S. Jarriault *et al.*, Signalling downstream of activated mammalian Notch. *Nature* **377**, 355–358 (1995).
41. P. Bagadia *et al.*, Bcl6-independent in vivo development of functional type 1 classical dendritic cells supporting tumor rejection. *J. Immunol.* **207**, 125–132 (2021).
42. I. Kwok *et al.*, Combinatorial single-cell analyses of granulocyte-monocyte progenitor heterogeneity reveals an early uni-potent neutrophil progenitor. *Immunity* **53**, 303–318.e5 (2020).
43. M. M. H. Li *et al.*, Interferon regulatory factor 2 protects mice from lethal viral neuroinvasion. *J. Exp. Med.* **213**, 2931–2947 (2016).
44. T. Matsuyama *et al.*, Targeted disruption of IRF-1 or IRF-2 results in abnormal type I IFN gene induction and aberrant lymphocyte development. *Cell* **75**, 83–97 (1993).
45. S. Hida *et al.*, CD8(+) T cell-mediated skin disease in mice lacking IRF-2, the transcriptional attenuator of interferon-alpha/beta signaling. *Immunity* **13**, 643–655 (2000).
46. T. Mizutani *et al.*, Homeostatic erythropoiesis by the transcription factor IRF2 through attenuation of type I interferon signaling. *Exp. Hematol.* **36**, 255–264 (2008).
47. B. Morgan *et al.*, Aiolos, a lymphoid restricted transcription factor that interacts with Ikaros to regulate lymphocyte differentiation. *EMBO J.* **16**, 2004–2013 (1997).
48. J. H. Wang *et al.*, Aiolos regulates B cell activation and maturation to effector state. *Immunity* **9**, 543–553 (1998).
49. F. J. Quintana *et al.*, Aiolos promotes TH17 differentiation by directly silencing Il2 expression. *Nat. Immunol.* **13**, 770–777 (2012).
50. L. Pasqualucci *et al.*, Mutations of the BCL6 proto-oncogene disrupt its negative autoregulation in diffuse large B-cell lymphoma. *Blood* **101**, 2914–2923 (2003).
51. X. Wang, Z. Li, A. Naganuma, B. H. Ye, Negative autoregulation of BCL-6 is bypassed by genetic alterations in diffuse large B cell lymphomas. *Proc. Natl. Acad. Sci. U.S.A.* **99**, 15018–15023 (2002).
52. U. Cytlak *et al.*, Ikaros family zinc finger 1 regulates dendritic cell development and function in humans. *Nat. Commun.* **9**, 1239 (2018).
53. D. Korenfeld *et al.*, STAT3 gain-of-function mutations underlie deficiency in human nonclassical CD16(+) monocytes and CD141(+) dendritic cells. *J. Immunol.* **207**, 2423–2432 (2021).
54. A. E. Moran *et al.*, T cell receptor signal strength in Treg and iNKT cell development demonstrated by a novel fluorescent reporter mouse. *J. Exp. Med.* **208**, 1279–1289 (2011).
55. S. L. Lee *et al.*, Unimpaired thymic and peripheral T cell death in mice lacking the nuclear receptor NGFI-B (Nur77). *Science* **269**, 532–535 (1995).
56. A. L. Dent, A. L. Shaffer, X. Yu, D. Allman, L. M. Staudt, Control of inflammation, cytokine expression, and germinal center formation by BCL-6. *Science* **276**, 589–592 (1997).
57. R. J. Johnston *et al.*, Bcl6 and Blimp-1 are reciprocal and antagonistic regulators of T follicular helper cell differentiation. *Science* **325**, 1006–1010 (2009).
58. S. Taki, S. Nakajima, E. Ichikawa, T. Saito, S. Hida, IFN regulatory factor-2 deficiency revealed a novel checkpoint critical for the generation of peripheral NK cells. *J. Immunol.* **174**, 6005–6012 (2005).
59. T. Sato *et al.*, Interferon regulatory factor-2 protects quiescent hematopoietic stem cells from type I interferon-dependent exhaustion. *Nat. Med.* **15**, 696–700 (2009).
60. S. Hida, M. Tadachi, T. Saito, S. Taki, Negative control of basophil expansion by IRF-2 critical for the regulation of Th1/Th2 balance. *Blood* **106**, 2011–2017 (2005).
61. D. Sakano *et al.*, BCL6 canalizes notch-dependent transcription, excluding mastermind-like1 from selected target genes during left-right patterning. *Dev. Cell* **18**, 450–462 (2010).
62. L. Tiberi *et al.*, BCL6 controls neurogenesis through Sirt1-dependent epigenetic repression of selective notch targets. *Nat. Neurosci.* **15**, 1627–1635 (2012).
63. S. Lukhele *et al.*, The transcription factor IRF2 drives interferon-mediated CD8+ T cell exhaustion to restrict anti-tumor immunity. *Immunity* **55**, 2369–2385.e10 (2022).
64. S. Morita, T. Kojima, T. Kitamura, Plat-E: An efficient and stable system for transient packaging of retroviruses. *Gene Ther.* **7**, 1063–1066 (2000).
65. K. W. O'Connor, C. Briseno, K. Murphy, Bcl6, Irf2 and Notch2 promote nonclassical monocyte development. Gene Expression Omnibus (GEO). https://www.ncbi.nlm.nih.gov/geo/query/acc.cgi?acc=GSE218504. Deposited 21 November 2022.